Simulation of seismic wave scattering for the computation of probabilistic coda-wave sensitivity kernels

Tuo Zhang[1,2], Christoph Sens-Schönfelder[1]
[1]GFZ German Research Centre for Geosciences, Potsdam, Germany
[2] Freie Universität Berlin, Berlin, Germany

EGU 2020-5408

Elastic Radiative Transfer Equations

The coupled radiative transfer equations for P- and S-waves in 2-D (Sens-Schönfelder et al. ,2009)

$$\left(\frac{\partial}{\alpha_0 \partial t} + \mathbf{n} \cdot \nabla\right) I_P(\mathbf{r}, \mathbf{n}, t) =$$

$$- \left(g_0^{PP} + g_0^{PS} + \frac{\omega}{\alpha_0 Q_P}\right) I_P(\mathbf{r}, \mathbf{n}, t)$$

$$+ \frac{1}{2\pi} \int_{2\pi} g^{PP}(\mathbf{n}, \mathbf{n}') I_P(\mathbf{r}, \mathbf{n}', t)\, d\mathbf{n}'$$

$$+ \frac{1}{2\pi} \int_{2\pi} g^{SP}(\mathbf{n}, \mathbf{n}') I_S(\mathbf{r}, \mathbf{n}', t)\, d\mathbf{n}'$$

$$\left(\frac{\partial}{\beta_0 \partial t} + \mathbf{n} \cdot \nabla\right) I_S(\mathbf{r}, \mathbf{n}, t) =$$

$$- \left(g_0^{SS} + g_0^{SP} + \frac{\omega}{\beta_0 Q_S}\right) I_S(\mathbf{r}, \mathbf{n}, t)$$

$$+ \frac{1}{2\pi} \int_{2\pi} g^{SS}(\mathbf{n}, \mathbf{n}') I_S(\mathbf{r}, \mathbf{n}', t)\, d\mathbf{n}'$$

$$+ \frac{1}{2\pi} \int_{2\pi} g^{PS}(\mathbf{n}, \mathbf{n}') I_P(\mathbf{r}, \mathbf{n}', t)\, d\mathbf{n}'$$

Spatially Variable Heterogeneity and Attenuation

$$P\left(m, \varepsilon^2(\mathbf{r})\right) = \frac{\varepsilon^2(\mathbf{r})}{\varepsilon_0^2} P\left(m, \varepsilon_0^2\right)$$

The right hand are rewritten as

$$- \left(g_0^{PP}(\varepsilon^2(\mathbf{r})) + g_0^{PS}(\varepsilon^2(\mathbf{r})) + \frac{\omega}{\alpha_0 Q_P(\mathbf{r})}\right) I_P(\mathbf{r}, \mathbf{n}, t)$$

$$+ \frac{1}{2\pi} \int_{2\pi} g^{PP}(\theta, \varepsilon^2(\mathbf{r})) I_P(\mathbf{r}, \mathbf{n}', t)\, d\mathbf{n}'$$

$$+ \frac{1}{2\pi} \int_{2\pi} g^{SP}(\theta, \varepsilon^2(\mathbf{r})) I_S(\mathbf{r}, \mathbf{n}', t)\, d\mathbf{n}'$$

and

$$- \left(g_0^{SS}(\varepsilon^2(\mathbf{r})) + g_0^{SP}(\varepsilon^2(\mathbf{r})) + \frac{\omega}{\alpha_0 Q_S(\mathbf{r})}\right) I_S(\mathbf{r}, \mathbf{n}, t)$$

$$+ \frac{1}{2\pi} \int_{2\pi} g^{SS}(\theta, \varepsilon^2(\mathbf{r})) I_S(\mathbf{r}, \mathbf{n}', t)\, d\mathbf{n}'$$

$$+ \frac{1}{2\pi} \int_{2\pi} g^{PS}(\theta, \varepsilon^2(\mathbf{r})) I_P(\mathbf{r}, \mathbf{n}', t)\, d\mathbf{n}'\ .$$

Monte Carlo Method

For numerically solving the radiative transfer equations we use the Monte Carlo method. The idea of the Monte Carlo method is based on the concept of wave packets or seismic phonons that carry in-formation about the wave energy but neglect phase information.

$$
\begin{aligned}
\Delta N_P(\mathbf{r},\mathbf{n},t) = \\
&- \Delta l \left(g_0^{PP}\left(\varepsilon^2(\mathbf{r})\right) + g_0^{PS}\left(\varepsilon^2(\mathbf{r})\right) + \frac{\omega}{\alpha_0 Q_P(\mathbf{r})} \right) N_P(\mathbf{r},\mathbf{n},t) \\
&+ \Delta l \int_{2\pi} g^{PP}\left(\theta,\varepsilon^2(\mathbf{r})\right) N_P(\mathbf{r},\mathbf{n}',t) \\
&+ \Delta l \int_{2\pi} g^{SP}\left(\theta,\varepsilon^2(\mathbf{r})\right) N_S(\mathbf{r},\mathbf{n}',t) \ .
\end{aligned}
$$

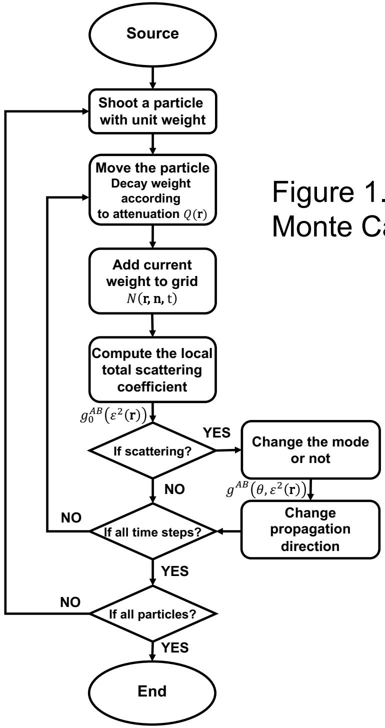

Figure 1.Flowchart of Monte Carlo simulation

Modelling with Spatially Variable Heterogeneity and Attenuation

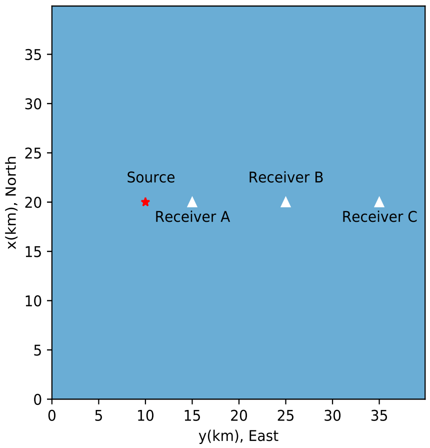

(a) Homogeneous

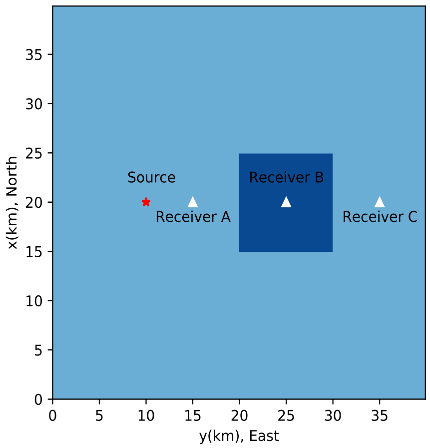

(b) Anomalous model

Figure 2. Illustrations of the model setup. (a) Homogeneous model with background ε= 0.05 and Q_P^{-1}= 0, Q_S^{-1}= 0 (simulation 1) and (b) Anomalous model with ε= 0.09(simulation 2) or intrinsic quality factors Q_P^{-1}= 0.17,Q_S^{-1}= 0.1 inside the anomaly (simulation 3). The background velocity of all models is Vp= 6km/s, Vs= 3.46km/s. The background density isρ= 2.7g/cc. The correlation length is a= 0.3km in all simulations. The red star indicates the source and three white triangles indicate receivers that are located before, within and behind the anomaly as seen from the source

Scattering Anomaly Simulation

The source emits pure P-wave energy

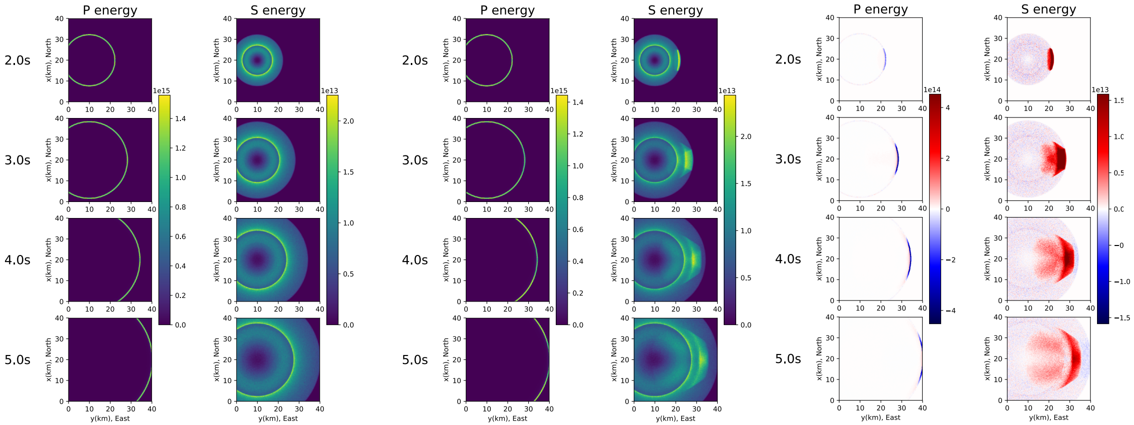

(a) uniform medium (b) medium with scattering anomaly (c) intensity differences

Figure 3.Snapshots (2s−5s) of the simulated wavefield in (a) the uniform medium and (b) the scattering anomaly medium. (c) differences between (a) and(b). Both the P energy and the S energy are recorded

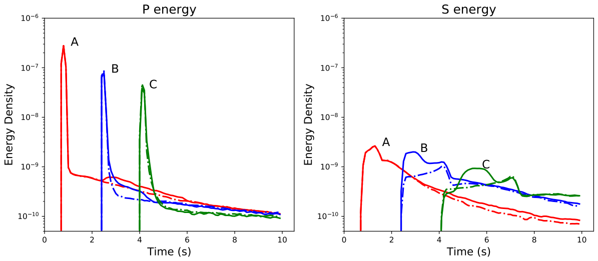

Figure 4.Envelopes at three receivers for the uniform medium (dotted) and the scattering anomaly medium (solid). The red, blue and green curves indicate the energy that arrives at the receiver A, B and C respectively.

GFZ
Helmholtz Centre
Potsdam

HELMHOLTZ

Scattering Anomaly Simulation

The source emits pure S-wave energy

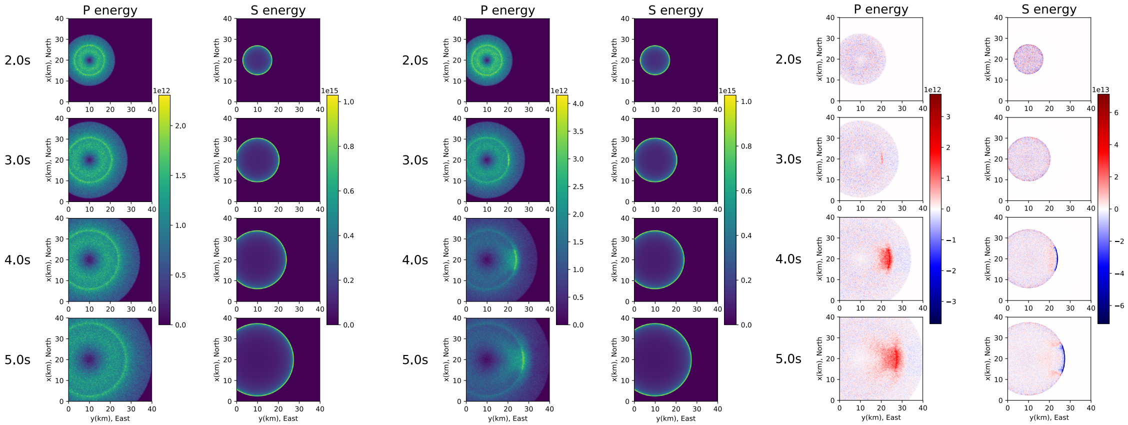

(a) uniform medium (b) medium with scattering anomaly (c) intensity differences

Figure 5.Snapshots (2s−5s) of the simulated wavefield in (a) the uniform medium and (b) the scattering anomaly medium. (c) differences between (a) and(b). Both the P energy and the S energy are recorded

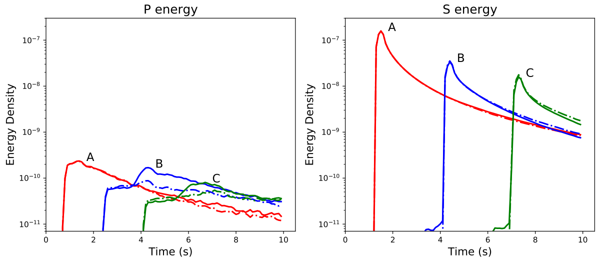

Figure 6.Envelopes at three receivers for the uniform medium (dotted) and the scattering anomaly medium (solid). The red, blue and green curves indicate the energy that arrives at the receiver A, B and C respectively.

Intrinsic Attenuation Anomaly Simulation

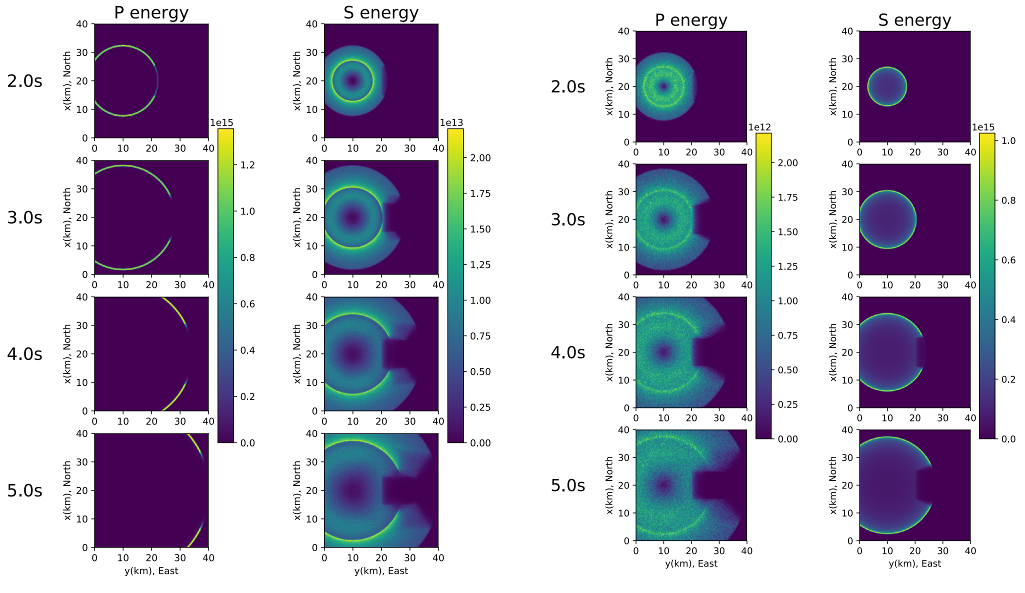

(a) P source

(B) S source

Figure 7.Snapshots (2s−5s) of the simulated energy field in the model with the anomaly in intrinsic attenuation. The intrinsic quality factors $Q_P^{-1}= 0.17, Q_S^{-1}= 0.1$, respectively.

The source is (a) P-wave and (b) S-wave. Both the P energy and the S energy are recorded.

Modelling the Specific Intensity

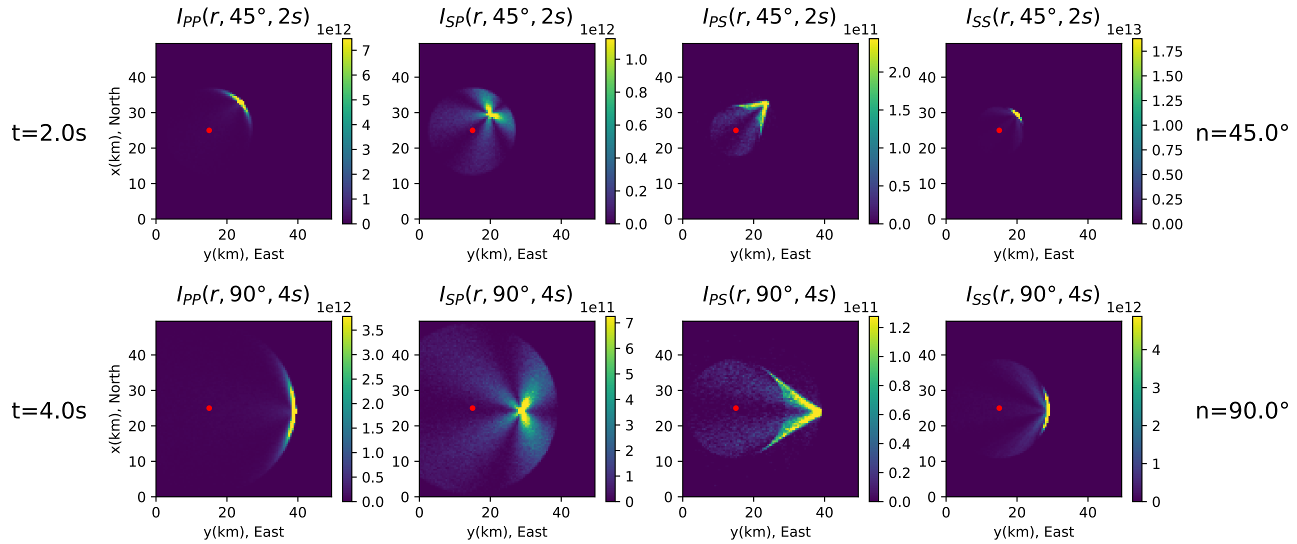

Figure 8.Snapshots (2s,4s) of the specific intensity $I_{Y\,X}(r, n, t)$ for propagation directions n= 45◦ and n= 90◦ in a uniform medium with background ε= 0.05. The red point indicates the source. Note that the maximum of the color scale for is clipped to avoid the high values of the ballistic energy.

Traveltime Sensitivity Kernels

The travel time shift for spatially distributed changes of P- and S-wave velocities:

$$\delta t_{YX}(t) = -\int_{V^d} [\frac{\delta\alpha}{\alpha}(\mathbf{r}')\,{}^{\alpha}K^{tt}_{YX}(\mathbf{r}',\mathbf{n}',t;\mathbf{r},\mathbf{r_0})+ \frac{\delta\beta}{\beta}(\mathbf{r}')\,{}^{\beta}K^{tt}_{YX}(\mathbf{r}',\mathbf{n}',t;\mathbf{r},\mathbf{r_0})]dV(\mathbf{r}')$$

$${}^{\alpha}K^{tt}_{YX}\,(\mathbf{r}',t;\mathbf{r},\mathbf{r_0}) = S^d \int_{S^d}\int_0^t \frac{I^{\dagger}_{PY}\,(\mathbf{r}',t-t',-\mathbf{n}';\mathbf{r})\,I_{PX}\,(\mathbf{r}',t',\mathbf{n}';\mathbf{r_0})\,dt'd\mathbf{n}'}{I_{YX}\,(\mathbf{r},t;\mathbf{r_0})}$$

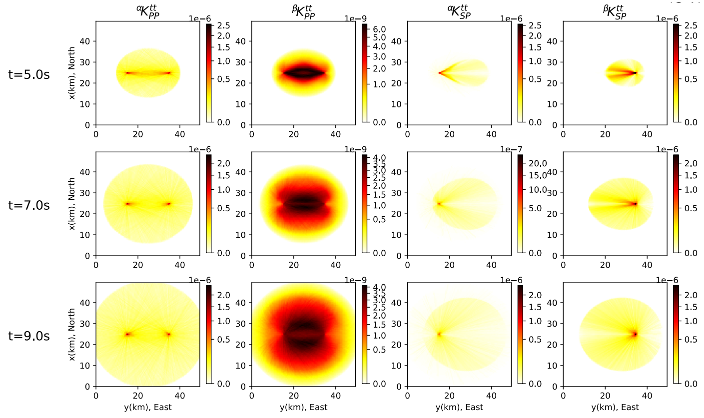

αKtt PP βKtt PP αKtt SP βKtt SP

$${}^{\beta}K^{tt}_{YX}\,(\mathbf{r}',t;\mathbf{r},\mathbf{r_0}) = S^d \int_{S^d}\int_0^t \frac{I^{\dagger}_{SY}\,(\mathbf{r}',t-t',-\mathbf{n}';\mathbf{r})\,I_{SX}\,(\mathbf{r}',t',\mathbf{n}';\mathbf{r_0})\,dt'd\mathbf{n}'}{I_{YX}X\,(\mathbf{r},t;\mathbf{r_0})}$$

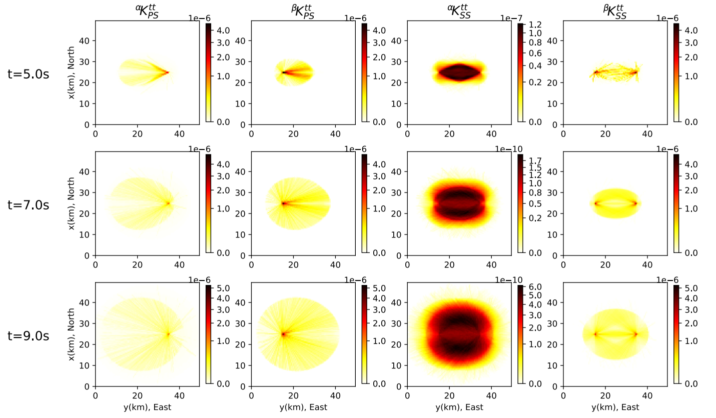

αKtt PS βKtt PS αKtt SS βKtt SS

Figure 9. Traveltime sensitivity kernels in uniform model at different lapse times.

Decorrelation Sensitivity Kernels

The decorrelation of the two wavefields recorded before and after the perturbation of the mechanical properties

$$dc_{YX}(t) = \frac{\delta I_Y(\mathbf{r}, t; \mathbf{r_0})}{2 I_{YX}(\mathbf{r}, t; \mathbf{r_0})}$$

$$= \frac{1}{2\varepsilon_0^2} \int_{V^d} \left| \delta\varepsilon^2(\mathbf{r}') \right| \ {}^{\varepsilon}K^{dc}_{YX}(\mathbf{r}', t; \mathbf{r}, \mathbf{r_0}) dV(\mathbf{r}')$$

$${}^{\varepsilon}K^{dc}_{YX}(\mathbf{r}', t; \mathbf{r}, \mathbf{r_0}) = S^d \sum_W \sum_V \int_{S^d} \int_{S^d} \int_0^t$$

$$\frac{c_W g_0^{VW}(\varepsilon_0^2) I^{\dagger}_{WY}(\mathbf{r}', t - t', -\mathbf{n}; \mathbf{r}) f_{VW}(\mathbf{n}, \mathbf{n}') I_{VX}(\mathbf{r}', t', \mathbf{n}'; \mathbf{r_0})}{I_{YX}(\mathbf{r}, t; \mathbf{r_0})}$$

$$dt' \, dn dn'$$

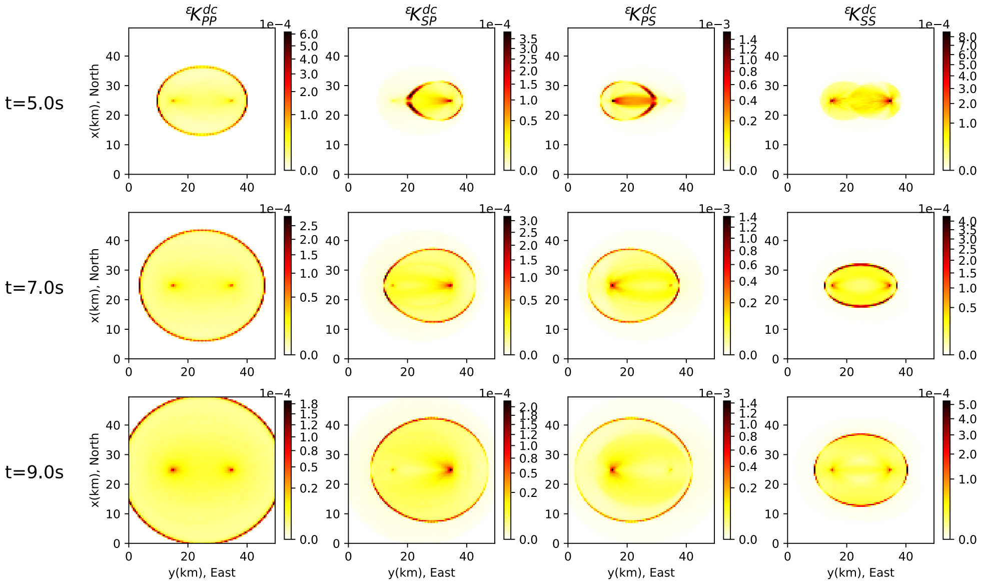

Figure 10. Decorrelation sensitivity kernels in uniform model at different lapse times.

Scattering Sensitivity Kernels

The perturbation of intensity in thecoda wave is written by

$$\frac{\delta I_{YX}}{I_{YX}}(\mathbf{r},t;\mathbf{r_0}) = \frac{1}{\varepsilon_0^2}\int_{V^d} \delta\varepsilon^2(\mathbf{r}')\,{}^{\varepsilon}K^{I}_{YX}(\mathbf{r}',t;\mathbf{r},\mathbf{r_0})dV(\mathbf{r}')$$

$$\begin{aligned}{}^{\varepsilon}K^{I}_{YX}(\mathbf{r}',t;\mathbf{r},\mathbf{r_0}) = {}^{\varepsilon}K^{dc}_{YX}(\mathbf{r}',t;\mathbf{r},\mathbf{r_0}) \\ -\left[\alpha_0(g_0^{PP}(\varepsilon_0^2)+g_0^{PS}(\varepsilon_0^2))\,{}^{\alpha}K^{tt}_{YX}(\mathbf{r}',t;\mathbf{r},\mathbf{r_0})\right. \\ \left.+\beta_0(g_0^{SP}(\varepsilon_0^2)+g_0^{SS}(\varepsilon_0^2))\,{}^{\beta}K^{tt}_{YX}(\mathbf{r}',t;\mathbf{r},\mathbf{r_0})\right]\end{aligned}$$

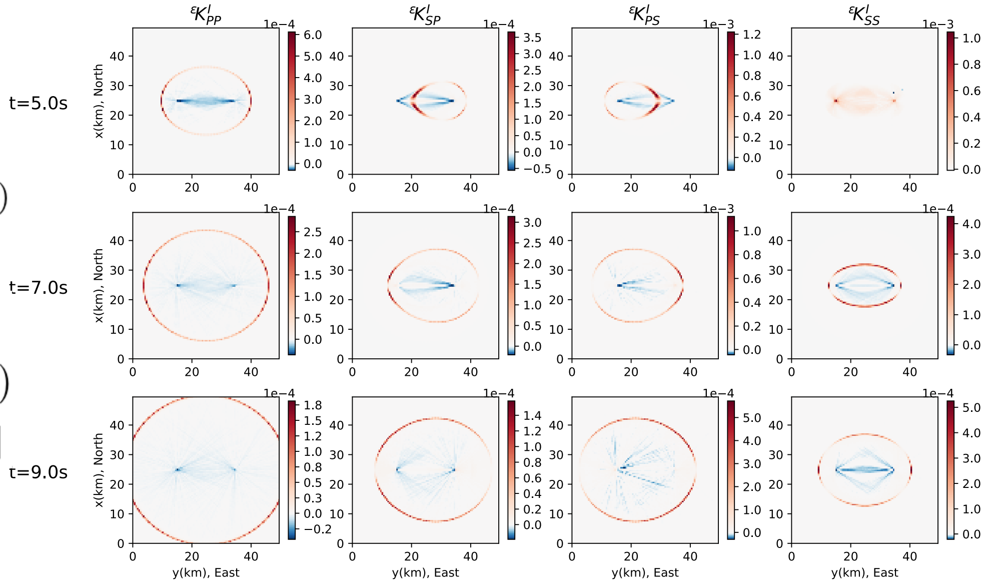

Figure 11. Scattering sensitivity kernels in uniform model at different lapse times.